Cell Metabolism
Article

Diet-Induced Obesity Causes Severe but Reversible Leptin Resistance in Arcuate Melanocortin Neurons

Pablo J. Enriori,[1] Anne E. Evans,[1] Puspha Sinnayah,[1] Erin E. Jobst,[1,4] Luciana Tonelli-Lemos,[1] Sonja K. Billes,[1] Maria M. Glavas,[1] Bernadette E. Grayson,[1] Mario Perello,[2] Eduardo A. Nillni,[2,3] Kevin L. Grove,[1] and Michael A. Cowley[1,*]

[1] Division of Neuroscience, Oregon National Primate Research Center, Oregon Health and Science University, Beaverton, OR 97006, USA
[2] Division of Endocrinology, Department of Medicine, Brown Medical School/Rhode Island Hospital, Providence, RI 02903, USA
[3] Department of Molecular Biology, Cell Biology, and Biochemistry, Brown University, Providence, RI 02903, USA
[4] School of Physical Therapy, Pacific University, Hillsboro, OR 97123, USA
*Correspondence: cowleym@ohsu.edu
DOI 10.1016/j.cmet.2007.02.004

SUMMARY

Despite high leptin levels, most obese humans and rodents lack responsiveness to its appetite-suppressing effects. We demonstrate that leptin modulates NPY/AgRP and α-MSH secretion from the ARH of lean mice. High-fat diet-induced obese (DIO) mice have normal ObRb levels and increased SOCS-3 levels, but leptin fails to modulate peptide secretion and any element of the leptin signaling cascade. Despite this leptin resistance, the melanocortin system downstream of the ARH in DIO mice is overresponsive to melanocortin agonists, probably due to upregulation of MC4R. Lastly, we show that by decreasing the fat content of the mouse's diet, leptin responsiveness of NPY/AgRP and POMC neurons recovered simultaneously, with mice regaining normal leptin sensitivity and glycemic control. These results highlight the physiological importance of leptin sensing in the melanocortin circuits and show that their loss of leptin sensing likely contributes to the pathology of leptin resistance.

INTRODUCTION

Obesity is defined as an excessive amount of body fat in relation to lean mass of sufficient magnitude to produce adverse health consequences. More than 60% of American adults are now overweight or obese, and the obesity prevalence in adults and children is growing dramatically (Zamboni et al., 2005). In most adults, body weight is relatively constant despite large variations in daily food intake and energy expenditure. Energy balance is regulated by neural and hormonal signals that are integrated in the brain (Seeley and Woods, 2003). Leptin, a hormone secreted primarily by adipocytes, is present in serum concentrations directly proportional to the amount of adipose tissue (Considine et al., 1996), signaling to the central nervous system (CNS) the relative extent of energy (adipose) stores in the body (Spiegelman and Flier, 2001).

Leptin regulates food intake by binding to CNS receptors and modulating the activity of neurons in appetite control centers in the brain (de Luca et al., 2005). In obese leptin-deficient mice, administration of leptin reduces hyperphagia and obesity. In contrast, obese mice that are deficient in the leptin receptor (ObRb) do not respond to leptin (Chen et al., 1996; Halaas et al., 1995). Leptin also affects energy expenditure in rodents and humans (Halaas et al., 1995; Rosenbaum et al., 2005). Activation of central ObRb increases sympathetic nervous system activity, which stimulates energy expenditure in adipose tissue (Commins et al., 1999).

The arcuate nucleus in the hypothalamus (ARH) is a major site of leptin sensing (Balthasar et al., 2004; Coppari et al., 2005; Cowley et al., 2001; van den Top et al., 2004). ObRb is highly expressed in the ARH (Elmquist et al., 1998; Schwartz et al., 1996). To access these receptors, peripheral leptin is transported across the blood-brain barrier to reach areas distal to circumventricular organs (Banks, 2003).

The ARH contains at least two key populations of leptin-responsive neurons that have opposite actions on food intake. One population expresses the anorexigenic peptide α-melanocyte-stimulating hormone (α-MSH), derived from the proopiomelanocortin (POMC) precursor. The other population expresses the orexigenic peptides, neuropeptide Y (NPY) and agouti-related peptide (AgRP) (Cone, 2005). Arcuate neurons subsequently innervate various second-order hypothalamic targets that express melanocortin-4 receptors (MC4R) and NPY receptors (Liu et al., 2003). Leptin can modulate both POMC and AgRP neurons and can promote the release of α-MSH, a potent anorexigen at central MC4Rs (Cowley et al., 2001; Elias et al., 1999; Schwartz et al., 1997).

Although most obese humans and rodents have very high amounts of circulating leptin, this hyperleptinemia neither reduces appetite nor increases energy expenditure. This state has been termed "leptin resistance." There

are only rare examples of single-gene mutations responsible for obesity in humans, and the majority of "normal" obesity is thought to be a consequence of polygenic interaction with the environment (Tschop and Heiman, 2001). Two hypotheses proposing mechanistic explanations for leptin resistance have received considerable attention: (1) failure of circulating leptin to reach its central targets (Banks, 2003); and (2) failure within components of the intracellular ObRb signaling cascade (Munzberg and Myers, 2005).

Mouse models of dietary obesity provide an excellent system to identify how leptin signaling becomes compromised when leptin resistance occurs. C57BL/6J mice fed a high-fat diet (HFD) exhibit increased body adiposity along with other characteristics of human obesity, such as diabetes mellitus (>70% of mice on HFD) (Burcelin et al., 2002). Notably, mice on HFD lose weight when the fat content of the diet decreases, independent of total calorie intake (Parekh et al., 1998). The development of obesity and leptin resistance in C57BL/6J mice on HFD can be divided into three stages. In the early stage, mice gain weight (adiposity) but maintain an adequate response to anorectic effects of peripheral leptin injection. In the middle stage, mice lose peripheral leptin sensitivity while retaining the capacity to respond to central leptin. Finally, in the late stage, mice demonstrate central leptin resistance (El-Haschimi et al., 2000).

Recently, it was shown that the expression of pStat3 (signal transducer and activator of transcription) in arcuate neurons was selectively reduced in leptin-treated diet-induced obese (DIO) mice but not in neurons within the VMH or DMH, suggesting that the ARH is a major site of leptin resistance. It was proposed that the increase of suppressor of cytokine signaling-3 (SOCS-3) levels may cause defective leptin signaling in the ARH of HFD mice (Munzberg et al., 2004). The heterozygous SOCS-3-deficient mouse was more sensitive to the weight-reducing effects of leptin and was resistant to the development of DIO (Howard et al., 2004). Moreover, using a SOCS-3 deficient (within the brain) mouse, Mori et al. showed that the level of POMC induced by leptin was greater in SOCS-3 deficient mice than in wild-type mice (Mori et al., 2004). These data indicate that SOCS-3 is a negative regulator of leptin-induced pStat3 signaling in the hypothalamus and that excessive activity of SOCS-3 may be a potential mechanism for leptin resistance.

We hypothesized that leptin sensitivity of POMC and NPY/AgRP neurons in the ARH is altered in male mice fed HFD. If so, we intended to explore the molecular mechanisms involved. Lastly, we wanted to determine if altered sensitivity could be restored when DIO mice lose weight after decreasing the fat content of their diet.

RESULTS

Effects of HFD on Body Composition: Body Weight, Fat Tissue, and Leptin Levels

At 20 weeks, mice fed HFD had a wide distribution in body weight gain showing bimodal characteristics. The heavier group on the HFD was named "diet-induced obese" (DIO) mice. Others on HFD remained almost as lean as controls, those fed regular chow (Figure 1A). We defined these as "diet-induced obese resistant" (DIO-R) mice, those with body weights ranging between the average ± 3 standard deviations of the control group. The small number of mice (~5%) that overlapped in the bimodal distribution of body weight was excluded from experiments. The frequency of DIO-R and DIO per cage was normally distributed, and the same ratio occurred when the mice were individually housed. Interestingly, initial body weight of identically aged mice significantly correlated to final weight and was the only factor that predicted DIO-R versus DIO (Figure S1 in the Supplemental Data available with this article online). No pre-existing differences to leptin sensitivity were seen between highest- and lowest-weight mice preceding HFD exposure; weight loss and decrease in food intake was similar with i.p. leptin (data not shown).

Over a period of 20 weeks, the DIO-R group became only 6.7% heavier than the control group, while the DIO group became 32.9% heavier (Figure 1B). The number of mice that became obese on the HFD steadily increased over time. By 13–15 weeks on HFD, ~65% of mice had become obese and this percentage remained stable past 20 weeks. At this point, the lean mass gain was similar for every group (control 6.7 ± 2.1 g, DIO-R 6.1 ± 1.1 g, DIO 8.0 ± 1.5 g). In contrast, fat gain was significantly different among the three groups. Control mice gained 1.7 g of fat and DIO-R mice gained 4.5 g of fat, ($p < 0.001$). The largest fat gain was obtained by the DIO group (10.5 g), around five times that of the control fat gain ($p < 0.001$). Thus, the extra weight gain in mice fed HFD was mostly due to accumulation of body fat. In parallel, leptin levels were elevated by 20 weeks on HFD and were significantly different between every group (control 3.7 ± 2.0 ng/ml, $n = 64$; DIO-R 14.3 ± 9.1 ng/ml, $n = 56$ and DIO 36.7 ± 10.0 ng/ml, $n = 58$, $p < 0.001$).

Effects of HFD on Food Intake

In DIO-R mice, calorie intake increased and paralleled that of control for the first 4 weeks; then, calorie intake decreased significantly from the fifth week until the end of the experiment. Although calorie intake in DIO mice was no different from the control, because of the different macronutrient composition of the diets, they were consuming significantly more fat (Figure 1C). Thus, obesity in C57BL/6J mice fed a HFD is not a result of hyperphagia but increased feeding efficiency (weight gained/kcal consumed) (Figure 1D).

Peripheral Leptin Effect on Food Intake and Body Weight after 20 weeks on HFD

We determined the minimum dose that could modify body weight or food intake in control mice (2 μg/g body weight for 2 days). After the second day of leptin injection, the control and DIO-R mice significantly lost weight. In contrast, the DIO group did not show any change in body weight (Figure 2A). Calorie intake after leptin treatment

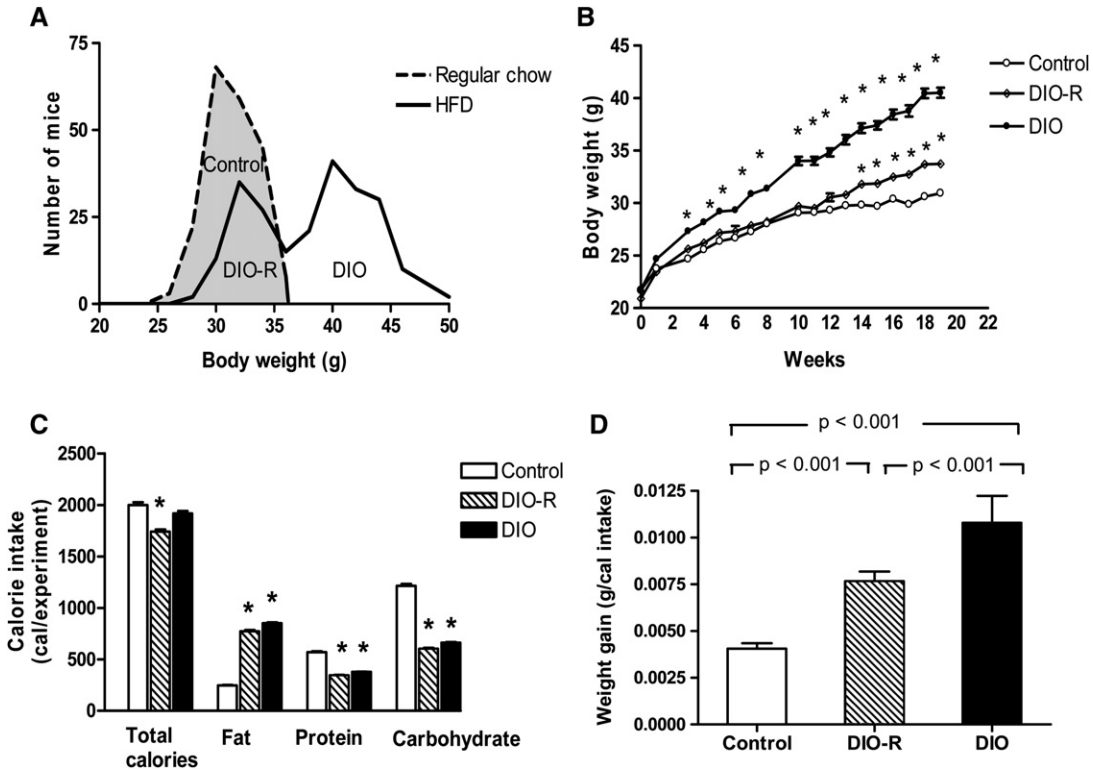

Figure 1. Body Weights and Feeding Characteristics for Mice Fed Regular Chow versus Mice Fed HFD

(A) Body weight distribution of control (12% fat diet) and DIO-R/DIO (45% fat diet) mice after 20 weeks. Normality test (DIO-R/DIO) was $p < 0.0001$.

(B) Body weight change of control, DIO-R, and DIO mice over 20 weeks. Results expressed as mean ± SEM (*$p < 0.001$).

(C) Total calorie, total fat, total protein, and total carbohydrate calorie intake for control, DIO-R, and DIO groups after 20 weeks.

(D) Feed efficiency (weight gained/kcal consumed) of control, DIO-R, and DIO groups.

Results expressed as mean ± SEM (*$p < 0.001$).

was reduced significantly in the control and DIO-R mice. However, no significant difference was found in the DIO group (Figure 2B). Two hours after i.p. leptin, leptin plasma concentrations in all groups were between 160–190 ng/ml. This represented a 40-fold increase from endogenous levels in control mice, a 12-fold increase in DIO-R mice, and a 5-fold increase in DIO mice ($p < 0.001$).

Central Leptin Effect after 20 Weeks on HFD

After i.c.v. leptin, control and DIO–R mice had a significant reduction of body weight at 24 hr. However, the DIO group showed no change (Figure 3C). Calorie intake after 24 hr was reduced by ~20% in control and DIO-R mice. No significant difference was found in the DIO group (Figure 2D). To confirm this lack of i.c.v. leptin responsiveness, we measured the immediate-early gene c-Fos (a marker of neuronal activation) in the ARH. After i.c.v. leptin, c-Fos expression significantly increased in control mice, but remained unchanged in DIO mice (data not shown).

Hypothalamic Secretion Experiment after 20 or 37 Weeks on HFD

We studied the baseline secretion of AgRP, NPY, and α-MSH from hypothalamic blocks. There was no difference in the baseline, nonstimulated secretion of NPY, AgRP, or α-MSH in DIO-R mice or DIO mice when compared with controls (Figure S2). Incubation with leptin caused a dose-dependent inhibition of AgRP and NPY secretion in the control group (EC50 = 23 nM, EC50 = 17 nM, respectively). The DIO-R group showed similar curves and similar EC50s (24 nM, 20 nM, respectively). On the contrary, AgRP and NPY secretion in the DIO group did not change with an increase in leptin concentration (Figures 3A–3F). The sensitivity of POMC neurons to leptin was studied by measuring α-MSH secretion. Incubation with leptin caused a dose-dependent increase of α-MSH levels in the control and DIO-R groups (EC50 = 46 nM, EC50 = 37 nM, respectively). The DIO group, however, was again resistant to the effects of leptin (Figures 3G–3I). We defined the α-MSH/AgRP secretion ratio as an index of activation of the MC4R. DIO-R mice had a 3-fold higher ratio of α-MSH to AgRP secretion than DIO mice (Figure 3J).

Peripheral Leptin Effect on ARH mRNA Expression after 20 Weeks on HFD

Since AgRP mRNA expression increases from rostral to caudal within the ARH (Wilson et al., 1999), neuropeptide

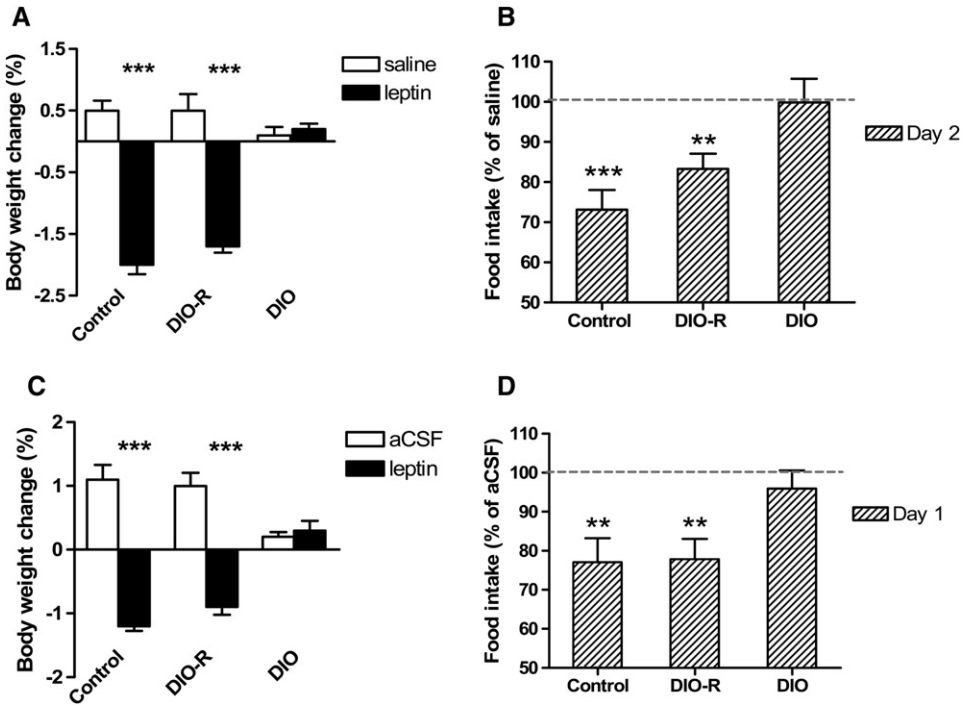

Figure 2. Effect of Peripheral and Central Leptin on Body Weight and Calorie Intake in Control, DIO-R, and DIO Mice

(A) Body weight change (%) 24 hr after i.p. saline or leptin (2 μg/g/day).

(B) Calorie intake 2 days after i.p. leptin (2 μg/g/day). Data from each group were normalized to their own saline control.

(C) Body weight change (%) 24 hr after i.c.v. aCSF or leptin (0.1 μg).

(D) Calorie intake 1 day after i.c.v. leptin (0.1 μg). Data from each group were normalized to their own aCSF control.

Results expressed as mean ± SEM (**$p < 0.01$, ***$p < 0.001$).

expression was divided into caudal and rostral regions for analysis. After i.p. leptin, caudal levels of AgRP expression were decreased by ~30% in both control and DIO-R mice. In contrast, DIO mice showed no expression changes (Figure 4A). Rostral areas of the ARH showed no differences in AgRP levels after leptin. Baseline levels of NPY expression were not significantly different between control and DIO groups. After leptin injection, NPY mRNA expression decreased 50% in control. There was no change in NPY mRNA expression in the DIO group (Figure 4B).

Neither baseline nor leptin-induced POMC mRNA expression was significantly different among groups when we considered the entire extent of the ARH or just rostral sections (Figure 4C). ObRb expression was not significantly different among groups in baseline levels (Figure 4D) nor after leptin injection (data not shown).

Synthesis of POMC-Derived Peptides in ARH

In order to test if the obesity-resistant phenotype (DIO-R) is due to a sustained level of anorexigenic POMC-derived peptides, we measured ACTH, CLIP, acetyl, and desacetyl-α-MSH. Desacetyl-α-MSH levels in DIO and DIO-R mice were significantly lower than control mice (Figure 4E). The same decrease of ACTH, CLIP, and acetyl α-MSH were also seen in DIO-R and DIO mice (Figure S2).

Peripheral Leptin Effect on ARH Signal Transduction after 20 Weeks on HFD

In order to assess leptin-induced activation of ARH cells, we measured c-Fos, phosphorylation of Stat3 (a well-known mediator of leptin activation) and pMAPK (a measure of the MAP Kinase pathway activation) in leptin-treated mice. Baseline conditions showed no significant differences among groups in the number of cells expressing c-Fos, pStat3, or pMAPK. After i.p. leptin, c-Fos expression in control and DIO-R groups increased significantly whereas there was no change in the DIO group (Figure 5A). pStat3 expression was dramatically increased in control and moderately elevated in the DIO-R leptin-treated group. No change was observed in the DIO group (Figure 5B). The control group showed a 2-fold increase in the positive pMAPK cells after leptin, whereas the DIO-R and DIO groups showed no difference (Figure 5C).

We measured SOCS-3 levels by ISH and real-time PCR in the ARH. Although the ISH data were inconclusive, we found higher levels of SOCS-3 mRNA in baseline conditions of DIO mice using real-time PCR. After i.p. leptin, control mice had elevated SOCS-3 levels while levels remained unchanged in DIO mice (Figure 5D).

Integrity of the Melanocortin Pathway

The unresponsiveness to leptin in DIO mice may be due to a primary insensitivity or a lack of secondary neuronal

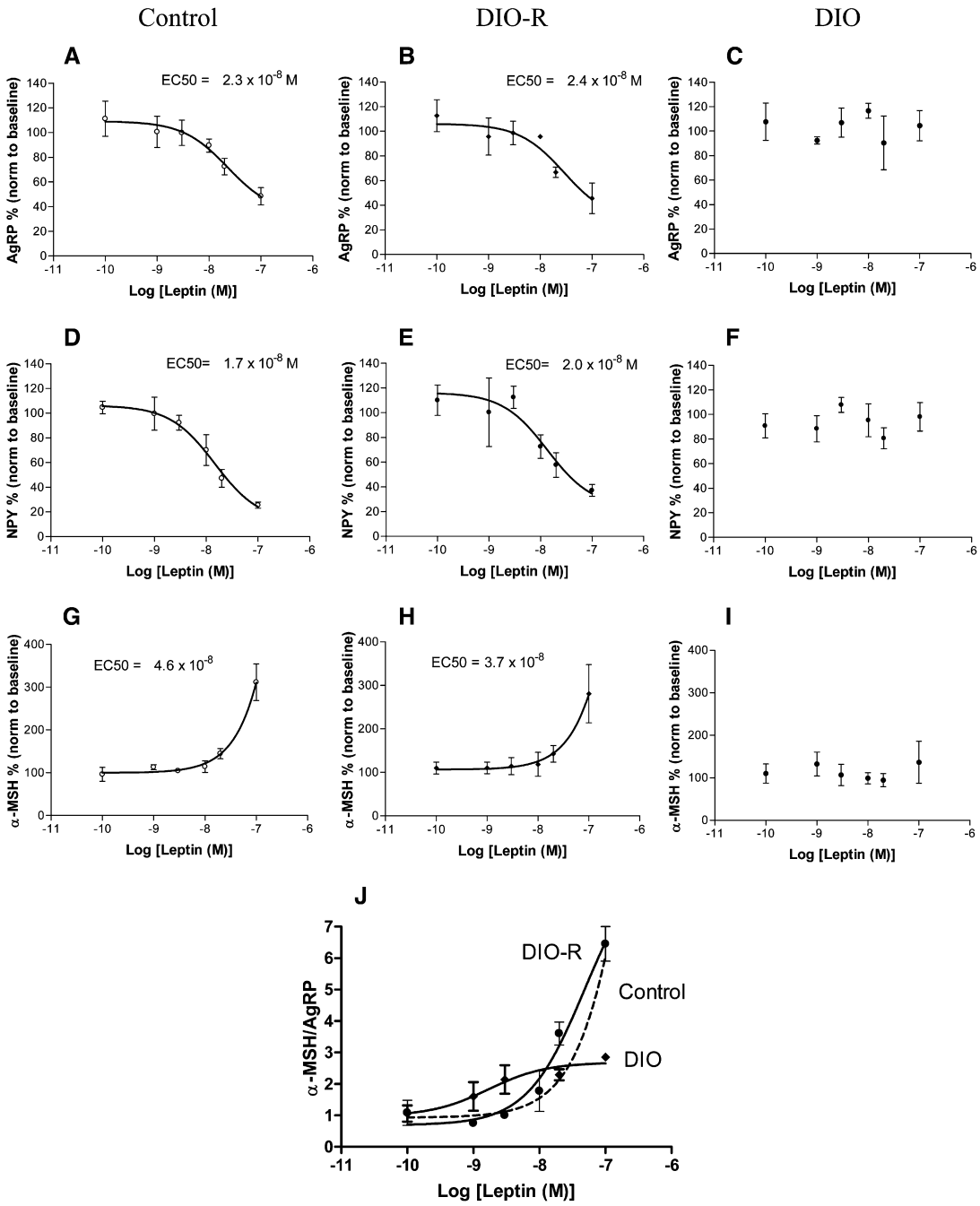

Figure 3. Leptin Modulation of Hypothalamic Neuropeptide Secretion in Control, DIO-R, and DIO groups

Data from each group were normalized to baseline levels. Figures represent four independent experiments.

(A–C) Leptin modulation of AgRP secretion.

(D–F) Leptin modulation of NPY secretion.

(G–I) Leptin modulation of α-MSH secretion.

(J) The α-MSH/AgRP ratio of secretion.

Results expressed as mean ± SEM ($p < 0.001$).

targets. The melanocortin pathway is a well-established pathway that mediates leptin's actions. We tested the hypothesis that the melanocortin system downstream of POMC neurons is intact by using a very low dose of MTII, a potent melanocortin agonist. One hour after i.p. MTII, calorie intake was reduced 45% in control, ~65% in DIO-R, and 90% in DIO. The orexigenic effect of MTII was maintained for 4 hr in control and DIO-R

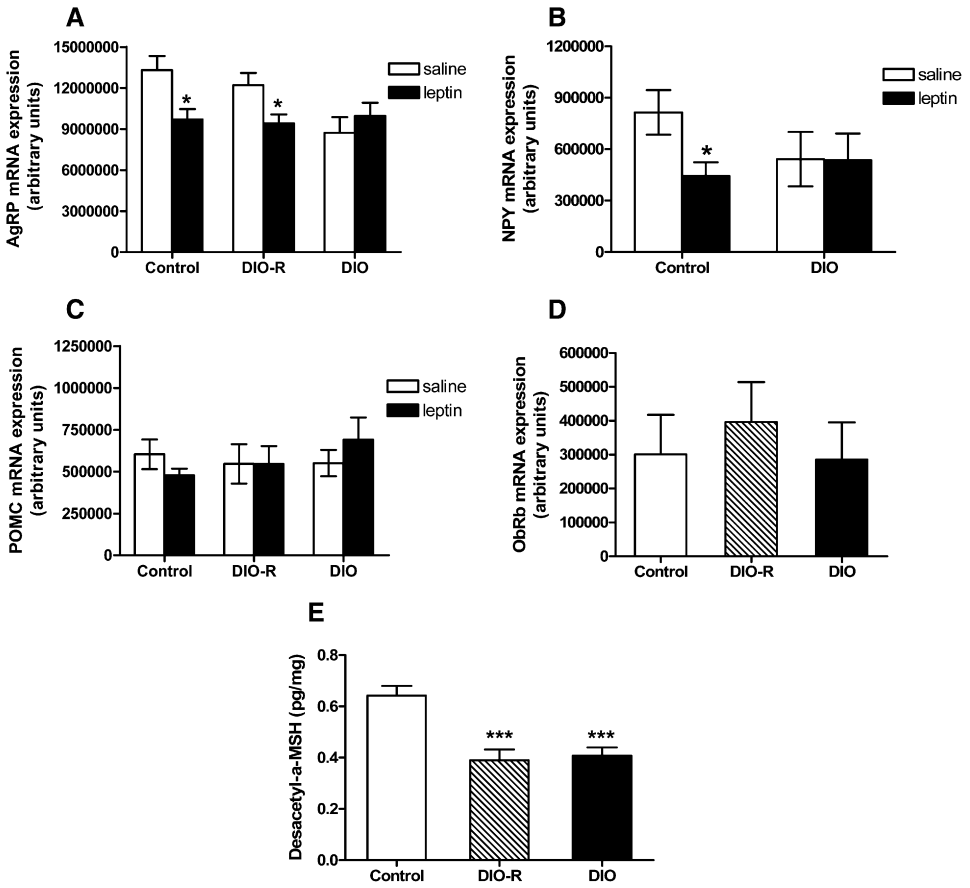

Figure 4. mRNA Neuropeptide Expression after i.p. Leptin, Expression of ObRb mRNA, and Concentration of Desacetyl-α-MSH in the ARH in Control, DIO-R, and DIO Groups

Results expressed as mean ± SEM (*$p < 0.05$, ***$p < 0.001$).

(A) Caudal AgRP mRNA expression after i.p. leptin (2 μg/g)/saline.

(B) Total NPY mRNA expression after i.p. leptin (2 μg/g)/saline.

(C) Total POMC mRNA expression after i.p. leptin (2 μg/g)/saline.

(D) Baseline ObRb expression.

(E) Desacetyl-α-MSH concentration.

groups and continued over 8 hr in the DIO group (Figure 6A).

When mice were given central MTII, they responded similarly to the peripheral injection: DIO mice showed a greater and prolonged response to MTII than control or DIO-R mice (data not shown). To determine if this exaggerated response in DIO mice was due to an upregulation of MC4R mRNA expression, we measured the expression in the PVH by ISH. Levels of MC4R mRNA were very low in control and DIO-R mice but were strikingly high in DIO mice (Figure 6B). We did an additional analysis of this gene expression by performing real-time PCR on microdissected PVH samples. The MC4R expression was significantly higher in DIO mice than in control mice ($p < 0.05$).

Restoration of Leptin Sensitivity after Changing from HFD to Regular Chow

To determine whether the effects of a HFD on energy balance were reversible, after 20 weeks on HFD, we continued one cohort of mice on HFD (DIO) and the other cohort was returned to regular chow diet (restored). Restored mice continuously lost weight and after ~7 weeks showed similar body weights to control (those maintained on regular chow during the whole experiment) (Figure 7A). Although total calorie intake of restored mice (weeks 20 to 37) was similar to that of DIO mice, total fat calorie intake was 5 times lower in the restored group ($p < 0.001$).

After 20 weeks on HFD, DIO mice were intolerant to glucose and insulin resistant. This intolerance and resistance worsened by 37 weeks, causing more than 70% of the mice to be diabetic. Mice were classified as diabetic when glucose AUC was 3 SD higher than the mean of control mice (Burcelin et al., 2002). At the end of 37 weeks, the restored group responded normally to glucose and insulin challenges (Figure 7B). Thus, the diabetes/obesity syndrome appears reversible at this stage.

We determined the leptin sensitivity of the restored group by injecting mice with leptin. After the second day

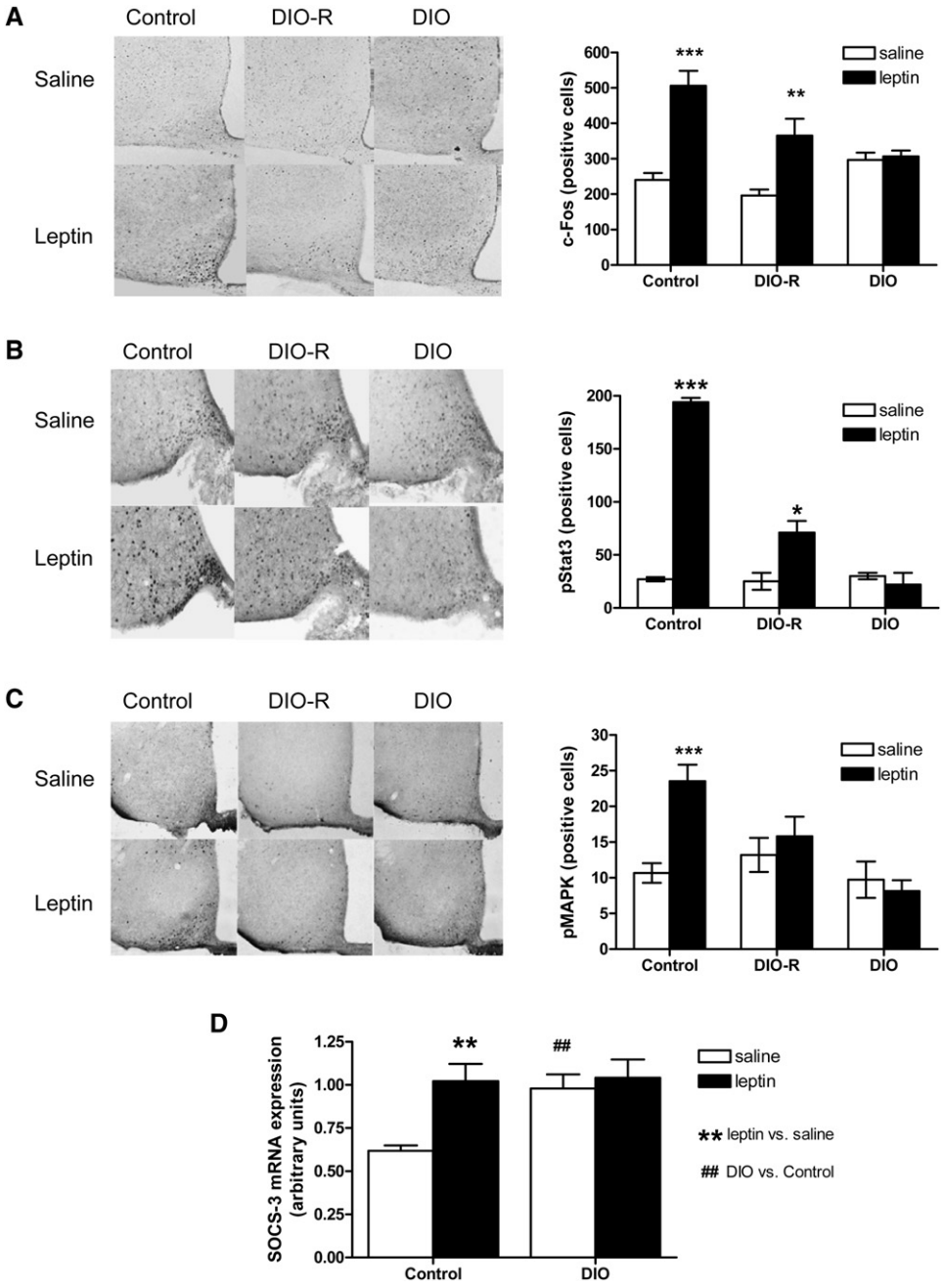

Figure 5. Effect of i.p. Leptin on Signal Transduction in the ARH

Results expressed as mean ± SEM. Representative microphotographs of hypothalamic sections are shown from control, DIO-R, and DIO groups (*$p < 0.05$, **$p < 0.01$, ***$p < 0.001$, $^{\#\#}p < 0.01$ saline control versus saline DIO).

(A) Expression of c-Fos 30 min after i.p. leptin (2 μg/g)/saline.

(B) Expression of pStat3 30 min after i.p. leptin (2 μg/g)/saline.

(C) Expression of pMAPK 30 min after i.p. leptin (2 μg/g)/saline.

(D) Expression of SOCS-3 mRNA 45 min after i.p. saline (2 μg/g)/leptin.

of i.p. leptin, body weight of the restored group was significantly reduced. This was identical to the sensitivity of the control group (Figure 7C). In addition, 100 nM leptin inhibited secretion of AgRP and NPY and stimulated secretion of α-MSH from hypothalamic explants in restored mice. In contrast, leptin did not modulate the secretion of AgRP, NPY, nor α-MSH from hypothalami of DIO mice (at 37 weeks) (Figures 7D, 7E, and 7F). These results show that sensitivity to leptin in the ARH was re-established in the restored group.

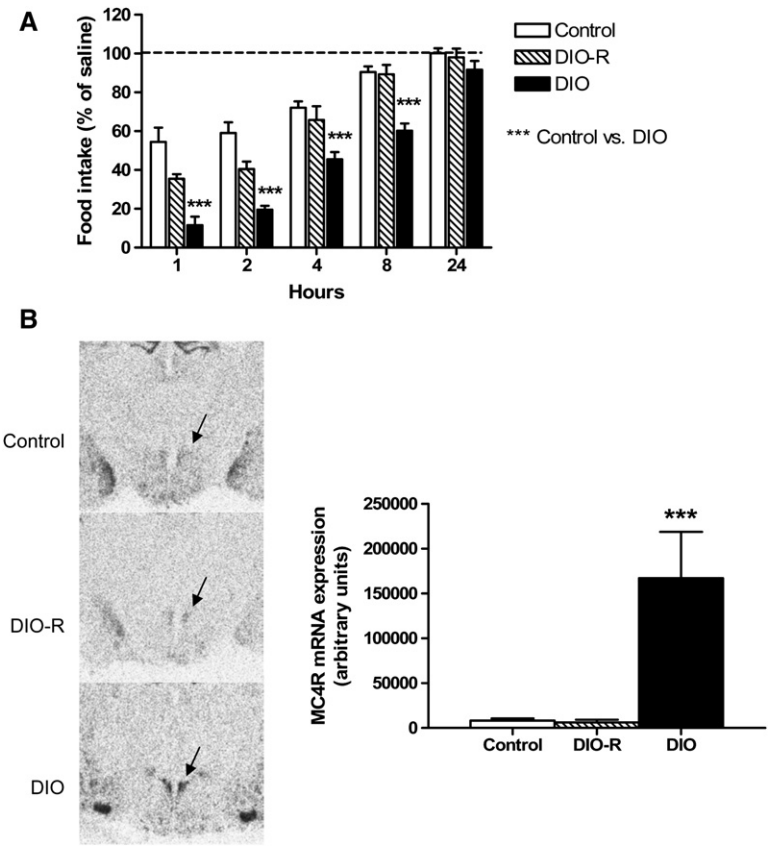

Figure 6. Melanocortin System Integrity

(A) Effect of i.p. MTII (1 μg/g) over 24 hr on food intake in control, DIO-R, and DIO groups. Data from each group normalized to their own saline control.

(B) Representative microphotograph and results of baseline MC4R mRNA expression in PVH of control, DIO-R, and DIO groups.

Results expressed as mean ± SEM (***$p < 0.001$).

DISCUSSION

Using a unique hypothalamic explant secretion assay, we demonstrate that leptin modulates NPY/AgRP and α-MSH secretion from the ARH in mice fed regular chow (control) and mice that remain lean when fed HFD (DIO-R). Leptin stimulated α-MSH secretion and inhibited NPY/AgRP secretion in a dose-dependent manner. On the contrary, leptin failed to modulate the secretion of melanocortin peptides in obese mice (DIO). We consider that this secretion comes from ARH neurons though we recognize the possibility that NPY secretion might be due to other neuron populations within the hypothalamus. Although previous studies have reported leptin's regulation of neuropeptide mRNA expression (Lin et al., 2000a; Wang et al., 2002), neuropeptide mRNA expression in a specific tissue does not necessarily correlate with the level of protein expression or the level of neuropeptide secretion. The first evidence of leptin-modulated neuropeptide secretion was demonstrated in primary hypothalamic cultures (Nillni et al., 2000). Others have analyzed neuropeptide content of rat CSF as a secretion index (Pritchard et al., 2003). Only a few studies address neuropeptide secretion by using hypothalamic slices. Li et al. showed that leptin treatment dose-dependently suppressed basal AgRP and NPY release in the hypothalamus of fasted male rats (Li et al., 2000). Recently, Breen et al. showed that hypothalamic slices treated with leptin significantly decreased AgRP release after depolarization with KCl, but revealed no change in POMC-derived peptide release (Breen et al., 2005). Here, we directly demonstrate that NPY/AgRP and α-MSH secretion in DIO mice is not modulated by leptin (in all doses studied).

DIO mice have increased adiposity and high plasma leptin concentrations, but the endogenous hyperleptinemia fails to curtail the progression of obesity. Moreover, DIO mice are unresponsive to peripheral or central leptin injection since they exhibit neither a decrease in food intake nor a decrease in body weight. This leptin resistance has also been shown by others (El-Haschimi et al., 2000; Lin et al., 2000b). Here, we specifically show leptin resistance in arcuate neurons in DIO mice. While c-Fos expression is induced in arcuate neurons of control and DIO-R mice after leptin treatment (presumably due to activation of POMC neurons (Elias et al., 1999)), leptin treatment does not alter c-Fos expression in arcuate neurons of DIO mice. The best-defined signal transduction pathway for leptin is the Janus kinase-STAT3 pathway. It is believed to be essential for mediating leptin's effects on homeostatic energy regulation (Bates et al., 2003). We show that once DIO is established, the ability of leptin to activate hypothalamic pStat3 signaling is also diminished. These data are in agreement with previous work (El-Haschimi et al., 2000; Munzberg et al., 2004). Notably, the dose of leptin we used to produce a response caused supraphysiological serum leptin levels (around 40-fold above

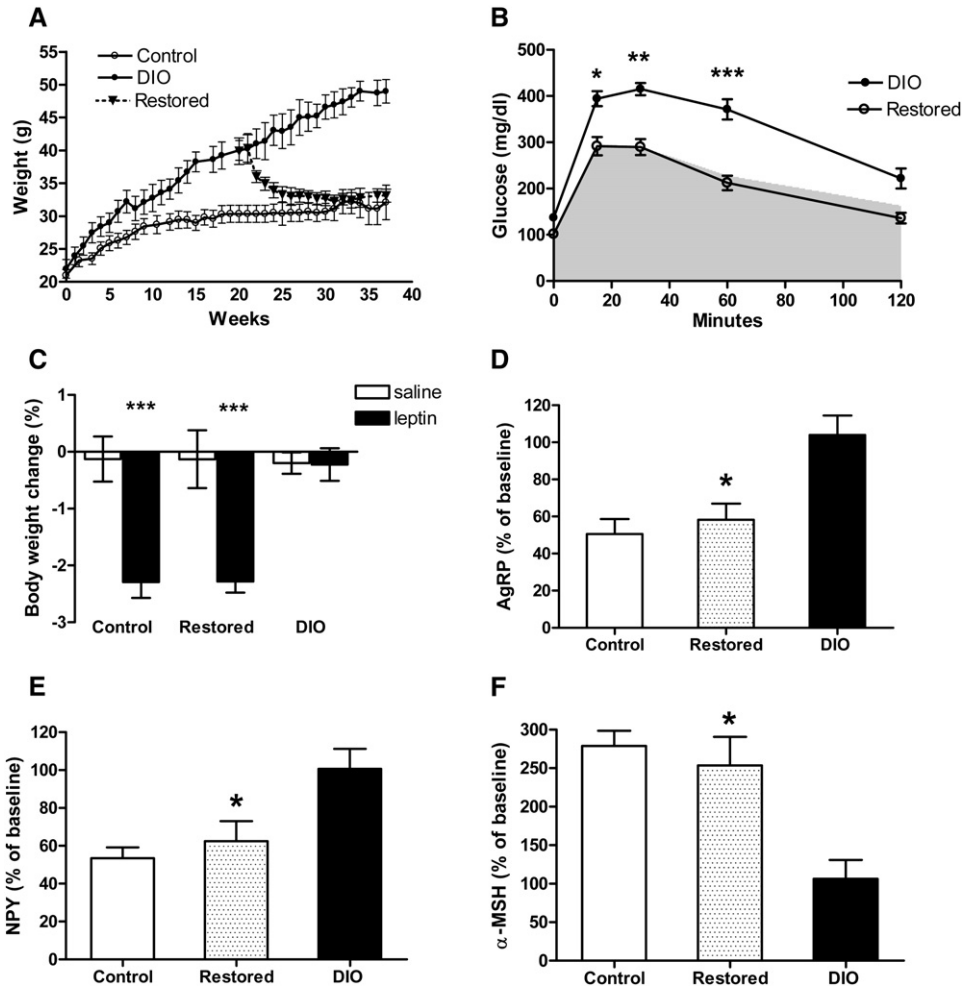

Figure 7. Restoration of Leptin Sensitivity after Changing from HFD to Regular Chow

(A) Body weight change of control, DIO, and restored mice at 37 weeks.

(B) Glucose tolerance in DIO and restored mice after 14 hr of fasting. Shaded region represents control group response.

(C) Body weight change (%) in control, restored, and DIO mice 24 hr after i.p. saline or leptin (2 μg/g/day).

(D) Leptin (100 nM) modulation of AgRP secretion in control, restored, and DIO groups. Data from each group normalized to baseline levels.

(E) Leptin (100 nM) modulation of NPY secretion in control, restored, and DIO groups. Data from each group normalized to baseline levels.

(F) Leptin (100 nM) modulation of α-MSH secretion in control, restored, and DIO groups. Data from each group normalized to baseline levels.

Results expressed as mean ± SEM (*$p < 0.05$, **$p < 0.01$,***$p < 0.001$).

endogenous control levels and 5-fold above DIO levels), suggesting that endogenous leptin signaling in the ARH of DIO mice must be severely impaired since they are unresponsive to such high leptin levels.

Our data does not support the hypothesis that hyperleptinemia produces leptin resistance by a down-regulation of ObRb, because ObRb mRNA expression was not different between control and DIO mice. These results agree with some studies in male mice and rats fed HFD (Munzberg et al., 2004; Sahu et al., 2002; Takahashi et al., 2002). However, other groups have shown decreased ObRb mRNA expression in these models (Lin et al., 2000b; Zhang and Scarpace, 2006). We consider that the magnitude of decreased ObRb expression, ~30% when it has been shown, is probably not enough to explain the leptin resistance phenotype. Sahu et al. showed that ObRb expression in rats remained unchanged despite adenovirus-mediated hyperleptinemia (Sahu et al., 2002).

We tested if leptin resistance might be due to a disruption downstream of leptin receptor binding. In normal rats, an induction of SOCS-3 (a negative regulator of leptin signal transduction) occurs following i.p. leptin in areas involved in body weight regulation (Bjorbaek et al., 1998). We found higher baseline SOCS-3 mRNA levels in the ARH of DIO mice. After i.p. leptin, only the control mice showed an increase of SOCS-3. These results are in agreement with others (Munzberg et al., 2004). Interestingly, deletion of SOCS-3 in POMC neurons caused a reduction in the rate of weight gain in mice fed HFD, and the

mutation had beneficial effects on glucose homeostasis (Kievit et al., 2006). The complete lack of leptin responsiveness of the ARH in DIO mice seems to possibly be due to increased SOCS-3 expression, yet cannot be proven by our current data. Deleting SOCS-3 in another neuronal population (e.g., AgRP) may help to provide more evidence supporting SOCS-3 as a major cause of leptin resistance.

To examine changes in neuropeptide expression with leptin treatment, we explored major ARH neurons involved in energy homeostasis. In control and DIO mice, NPY, AgRP and POMC mRNA expression were not different in baseline conditions, as previously shown (Takahashi et al., 2002). After leptin, NPY and AgRP mRNA expression decreased in control mice, but had no effect on DIO mice. We anticipated this result, since the secretion experiment showed decreased release only in the control mice. Many groups have achieved similar and dissimilar results. However, all of the groups' paradigms differed slightly from our own (Lin et al., 2000a; Wang et al., 2002).

It is well-established that the melanocortin pathway mediates some of leptin's actions. Since α-MSH is a MC4R agonist and AgRP is a MC4R inverse agonist, the secretion ratio α-MSH/AgRP is an index of MC4R activation. Here we show that at most leptin concentrations, DIO mice have 3 times less activation of this receptor compared with control or DIO-R mice. The DIO's leptin resistance prevents a leptin-induced increase of α-MSH secretion while preventing a decrease in AgRP secretion. This leads to weakened central melanocortin activation. We confirmed that the distal components of the melanocortin system were intact. Indeed, in DIO mice the MC4R agonist caused a prolonged effect of reduced feeding, as seen by others (Pierroz et al., 2002). We consider that this increased responsiveness is due to the observed overexpression of MC4R mRNA seen in the PVH of DIO mice. While one group also showed increased expression of MC4R in the VMH and other areas in DIO mice (Huang et al., 2003), another group found a lower MC4R expression in DIO rats. However, the latter group demonstrated the same response to MTII treatment as our results (Li et al., 2004). Thus, leptin resistance leads to some type of hypersensitivity in the melanocortin pathway in response to pharmacological stimulation of the MC4R, at least partially caused by an overexpression of MC4R. This series of studies strongly suggests a primary failure of leptin to modulate the melanocortin system in DIO mice, and further suggests that the distal melanocortin system remains intact and capable of regulating energy balance.

Despite genetically identical backgrounds, some C57BL/6J mice on HFD are able to maintain a regular body weight—only 7% heavier than control mice. DIO-R mice also retain the same "normal" response to exogenous leptin and glycemic control as control mice. The ability of DIO-R mice to maintain their regular body weight is not due to overexpression of melanocortin peptides, because there was a decrease in the biosynthesis of prohormones (acetyl- and desacetyl-α-MSH, ACTH, and CLIP). We found that the only predictor of DIO-R versus DIO mice was that initial body weights (at 6 weeks of age) significantly correlated to final body weights. Variations in litter size could have been the cause, since litter size can have strong effects on development of adiposity (Schmidt et al., 2000). Levin and colleagues did extensive work on diet resistance and diet-induced obese animals using a selective inbred strain of rats (Irani et al., 2007; Levin et al., 1997). These rats showed pre-existing differences to leptin/insulin sensitivity and other metabolic parameters before HFD exposure. We did not see such differences in the homogenous in-bred strain of C57BL/6J mice we used. Koza et al., however, used the same mouse model as ours and was able to determine gene expression differences in the adipose tissue before the mice were put on HFD. They also showed that these mice, prone to DIO, have a stable phenotype that can be detected soon after weaning. Furthermore, they suggest an epigenetic mechanism underlying the variable obesity phenotypes (Koza et al., 2006).

DIO mice become leptin resistant and most of them become diabetic. But, they can lose weight by decreasing the fat content of their diet (Parekh et al., 1998). In our model, the restored group lost weight by eating the same amount of calories as the DIO group, but less fat. The mice of Koza et al. showed the same response as the first 2 weeks of our 7 week diet reversal (Koza et al., 2006). This suggests that it is macronutrient composition that causes weight gain in DIO mice and not the total calories consumed. After losing weight, the response to a glucose challenge was normalized, as well as leptin sensitivity, shown by a decrease in body weight after i.p. leptin. Restored mice showed a re-established response to leptin-regulated neuropeptide secretion. This recovery of leptin sensitivity was in parallel with the recovery of NPY/AgRP and POMC neurons' response to leptin actions.

In summary, we determined that leptin sensitivity of POMC and NPY/AgRP neurons in the ARH is drastically decreased in DIO, but not in DIO-R mice. While we have excluded the possibility that changes in ObRb expression could be responsible for leptin resistance, the observed upregulation of SOCS-3 supports the hypothesis that it may be playing a key role. We demonstrated that the melanocortin system downstream of the ARH in DIO mice is over-responsive possibly due to upregulation of MC4R in the PVH. Lastly, we demonstrated that the recovery of leptin resistance is due to a recovery of NPY/AgRP and POMC neuron sensitivity to leptin's actions. These studies strongly suggest a primary failure of leptin to modulate the melanocortin system in DIO mice, and further suggest that the distal melanocortin system remains intact and capable of regulating energy balance. These studies do not prove that leptin resistance in the ARH is a cause of DIO, but they strongly support the case since it is known that leptin sensing in the melanocortin circuits is necessary for normal energy homeostasis (Coppari et al., 2005). Our work suggests that therapeutic strategies to inhibit SOCS-3, to regulate the melanocortin system, or to directly stimulate MC4R may bypass leptin resistance in obese organisms.

EXPERIMENTAL PROCEDURES

Animals: Diet and Experimental Procedures

At 6 weeks of age, C57BL/6J mice (Jackson Laboratories, Bar Harbor, ME) were fed a regular diet (Purina Lab Chow #5001, Ralston Purina Corp, St. Louis, MO) or a HFD (Rodent Chow #D12451, Research Diets Inc., New Brunswick, NJ) for 20 or 37 weeks. Regular diet provided 3.3 kcal/g of energy (59.8% carbohydrate, 28.0% protein, and 12.1% fat). HFD provided 4.75 kcal/g of energy (35.0% carbohydrate, 20.0% protein, and 45.0% fat). In seven independent experiments, mice were housed (5/cage) in a controlled environment. Food and water were available ad libitum unless otherwise indicated. Body weights were measured weekly. To measure food intake, some mice were individually housed. In two experiments, groups of DIO mice that had been on HFD for 20 weeks were then switched to regular diet for 17 weeks (until week 37). Mouse procedures were performed in accordance with the guidelines and approval of the Oregon National Primate Research Center's Institutional Animal Care and Use Committee. Body composition was measured using dual X-ray absortiometry (DXA) (Lunar Piximus, GE Medical Systems, Madison, WI).

Radioimmunoassay

α-MSH immunoreactivity was measured with a rabbit anti-α-MSH (Phoenix Pharmaceuticals, Inc., Belmont, CA). The antibody cross-reacts fully with the acetylated α-MSH and partially (46%) with desacetylated α-MSH, but not with NPY nor AgRP. NPY immunoreactivity was measured with a rabbit anti-NPY (kindly provided by Dr. Williams, University of Liverpool, UK). The antibody does not crossreact with AgRP nor α-MSH (King et al., 2000). AgRP immunoreactivity was measured with a rabbit anti-AgRP (82-131)-NH2 (Phoenix Pharmaceuticals, Inc., Belmont, CA). The antibody does not crossreact with α-MSH nor NPY. ^{125}I-labeled α-MSH, AgRP, and NPY were prepared by the iodogen method and purified by high-pressure liquid chromatography (α-MSH and NPY) or by AG1X8 ion exchange resin (AgRP) (University of Mississippi Peptide Radioiodination Service Center, University, MS). For the α-MSH RIA, the lowest detectable level (LDL) that could be distinguished from the zero standard was 0.30 fmol/tube. The intra-assay variation ($CV\%_1$) was determined by replicate analysis (n = 10) of two samples at α-MSH concentrations of 2 and 10 fmol/tube, and the results were 7.8% and 7.5%, respectively. The inter assay-variation ($CV\%_2$) was 10.7% and 12.1% for the range of value measured. For NPY, the LDL was 0.32 fmol/tube. The $CV\%_1$ was determined by replicate analysis (n = 10) of one sample at a NPY concentration of 5 fmol/tube and the result was 9.1%. The $CV\%_2$ was 11.1%. For AgRP, the LDL was 0.70 fmol/tube. The $CV\%_1$ was determined by replicate analysis (n = 10) of two samples at AgRP concentrations of 2 and 10 fmol/tube, and the results were 9.1% and 9.8%, respectively. The $CV\%_2$ was 13.4% and 13.5% for the range of values measured.

Intraperitoneal Leptin in Mice before and after 20 or 37 Weeks on HFD

Mice (28 control, 10 DIO-R, and 10 DIO) were individually housed and sham injected for 5 days prior to drug treatment. Mice were divided into two groups which received intraperitoneal (i.p.) injections of recombinant murine leptin (Peprotech, 2.0 μg/g body weight) or saline for 2 days. Body weights and calorie intake were measured daily.

Intraperitoneal Melanotan-II in Mice after 20 or 37 Weeks on HFD

Mice (8 control, 8 DIO-R, and 8 DIO) were individually housed and fasted overnight. Following 5 days of daily sham injection, half of the mice received i.p. melanotan-II (MTII) (NeoMPS Inc., San Diego, CA, 1.0 μg/g) and the other half received i.p. saline. Fifteen minutes after the injection, food was reoffered. Food intake was measured during 24 hr after the injection.

Intracerebroventricular Leptin/MTII in Mice after 20 Weeks on HFD

Under isoflurane anesthesia, a sterile guide cannula (15 mm long, 22 gauge, Plastics One, Inc. Roanoke, VA) was stereotaxically implanted into the lateral ventricle (-0.5 mm posterior, 1 mm lateral to bregma, and 1.5 mm below the surface of the skull, in accordance with Franklin and Paxinos [Paxinos and Franklin, 2001]) of control, DIO-R, and DIO mice. A 28-gauge obturator was inserted into each cannula. Cannula position was verified at the end of the experiment by dye administration and histological analysis. After ~2 weeks, mice received intracerebroventricular (i.c.v.) leptin (0.1 μg) or aCSF in 1 μl. In one experiment, food intake and body weight were measured after 24 hr. Two days later, experimental treatments were crossed over in all mice. In another experiment, mice were perfused 45 min after i.c.v. leptin administration for IHC.

Eight naïve mice were given increasing doses of MTII i.c.v. (0.01–500 ng). The minimum dose that produced significant modification of food intake in control mice (0.1 ng) was selected for the follow-up experiment. Mice (control, DIO-R, and DIO) were divided into two groups, each receiving i.c.v. MTII or aCSF after an overnight fast. Food intake was recorded during 24 hr after the injection.

Static Incubation of Hypothalamic Explants after 20 or 37 Weeks on HFD

After 20 weeks on regular or HFD diet, in five duplicate experiments, 620 mice were sacrificed by decapitation and whole brains immediately removed. The hypothalamus was cut from the rest of the brain. Care was taken to ensure that there was no contamination of the hypothalamic portion with residual pituitary. A 2 mm thick slice of mediobasal forebrain was prepared using a vibrating microtome (Leica VS 1000, Leica Microsystems, Inc., Bannockburn, IL). Each slice was taken from the base of the brain to include the PVH and ARH. Hypothalami were treated separately with aCSF (w/0.6 TIU aprotinin/ml), equilibrated with 95% O_2 and 5% CO_2 and incubated at 37°C. After a 1 hr equilibration period, hypothalami were incubated for 45 min in aCSF (basal period) before being challenged with a single concentration of leptin (0.1 to 100 nM) for 45 min. Tissue viability was verified by exposure to 56 mM KCl for 45 min. Each experiment was repeated four times. Treatments were performed in quadruplicate. At the end of each period, supernatants were removed and frozen until assayed. Hypothalamic explants that failed to show peptide release 3X above that of basal in response to KCl were excluded from analysis.

Immunohistochemical Studies after 20 Weeks on HFD

Mice (8 control, 8 DIO-R, and 9 DIO) were injected i.p. with 2 μg/g leptin or saline. After 30 min, mice were killed under pentobarbital anesthesia by cardiac perfusion with PBS then paraformaldehyde in $NaPO_4$ buffer (pH 7.4). Brains were removed, dehydrated in 25% sucrose, frozen and stored at −80°C until sectioned coronally on a microtome (30 μm). For pStat3 and pMAPK immunohistochemical (IHC), free-floating tissue was pretreated in 1% NaOH+1% H_2O_2 in H_2O for 10 min, 0.3% glycine for 10 min, 0.03% SDS for 10 min, and blocked in 3% NDS in PBS/0.25% Triton X-100/0.02% NaN_3. For c-Fos IHC, tissue was incubated in blocking buffer for 20 min (KPBS+0.4% Triton X-100 + 2% donkey serum) to reduce background. Antibodies (Phospho-Stat3 rabbit #9135, 1:1000, Phospho-p44/42 Map Kinase rabbit #9101, 1:1000, Cell Signaling Technology, Beverly, MA; c-Fos rabbit #SC-52, 1:10000, Santa Cruz Biotechnology, Inc., Santa Cruz, CA) were added in blocking solution and incubated overnight at room temp. Sections were washed, incubated with Biotin-SP-conjugated AffiniPure $F(ab^1)_2$ Fragment Donkey Anti-Rabbit IgG secondary antibody (Jackson ImmunoResearch Laboratories, West Grove, PA) 1:1000 in blocking solution, without NaN_3, for 1 hr. Tissue was treated with Vectastain Elite ABC Kit (Vector Labs, Burlingame, CA) for 1 hr, and the signal developed by $NiSO_4$/DAB solution. Tissue was mounted on subbed slides, cover slipped, and photographed.

In Situ Hybridization after 20 Weeks on HFD

Mice (23 control, 21 DIO-R, and 22 DIO) were injected i.p. with 2 μg/g leptin or saline. After 2 hr, mice were killed and brains were frozen on dry ice. In situ hybridization (ISH) was performed as previously described (Grove et al., 2001). Six riboprobes were transcribed from cDNA as follows: rat NPY cRNA (400 bp) and rat POMC cRNA (925 bp), in which 25% of the UTP was ^{35}S-labeled, and mouse AgRP cRNA (807 bp), rat leptin receptor (ObRb) cRNA (~400 bp), mouse MC4R cRNA (~520 bp) and SOCS-3 cRNA (450 bp) in which 100% of the UTP was ^{33}P-labeled (AgRP, ObRb, MC4R, and SOCS-3 cDNAs were all kind gifts from the Elmquist Lab). Tissue was incubated in antisense probe (20 million counts per ml labeled probe) overnight at 55°C. Tissue was then washed in SSC, RNase A at 37°C, then 0.1x SSC at 55-60°C. Tissue was dehydrated and exposed to autoradiographic film for 1–8 days then dipped in Kodak NBT2 emulsion and stored in light-tight boxes for 7–60 days. Slides were developed and counterstained with cresyl violet. A CoolSnap HQ camera (Photometrics, Westchester, PA) coupled with Metamorph Software (Universal Imaging Corp) was used to quantify autoradiograms. The area of exposed film and the average gray level density of labeling (integrated OD) in each region studied were measured using a constant sampling box encompassing the entire labeled area. Background labeling was subtracted from OD values. For the PVH and ARH measurements, the sampling box encompassed the entire nucleus, except for the SOCS-3 sampling box which contained 1 hemisphere of the ARH. Mean integrated OD for each brain region was obtained from sections that were anatomically matched between mice.

Microdissection and Real-Time PCR after 20 Weeks on HFD

Mice (14 control and 14 DIO) were injected i.p. with 2 μg/g leptin or saline. After 45 min, mice were anesthetized and brains were rapidly removed. The hypothalamus was cut from the rest of the brain. 0.4 mm-slices were prepared in aCSF using a vibrating microtome and then placed in RNAlater (Ambion, Austin, TX). Using a dissecting microscope, the ARH and PVH were cut from each slice using the fornix, optic tracts, and third ventricle as landmarks. ARH and PVH pieces were then put into separate microcentrifuge tubes and stored at −80°C. Total RNA was isolated from each sample using Qiagen's RNeasy Mini Kit (Valencia, CA). Standard RT-PCR was performed using 0.1 μg of total RNA. Samples were bioanalyzed on a RNA 6000 Nano chip kit (Agilent 2100 Bioanalyzer, Agilent Technologies, Inc., Palo Alto, CA) to check for integrity and concentration. Real-time PCR was performed on the ABI 7900HT (Applied Biosystems Foster City, CA) using the SOCS-3 and MC4R primer/probe set (cat. #mm00545913 s1, #mm 00457483 s1, ABI) for 45 cycles and using 18S as an internal control.

Glucose/Insulin Tolerance Tests after 20 or 37 Weeks on HFD

After a 14 hr fast, samples were obtained in the morning from saphenous vein bleeds. Blood glucose was measured using a glucometer (Accu-chek, Roche Diagnostic Corporation, Indianapolis, IN) at 0, 15, 30, 60 and 120 min after an i.p. injection of glucose (1 mg/g). Samples (30 μl of blood) were obtained at each time point to check for insulin levels by RIA (Linco Research Inc). For the insulin tolerance test (ITT), blood glucose measurements were taken at 0, 15, and 30 min after injection of human insulin (1.0 U/kg; Lilly, Indianapolis, IN).

HPLC Fractionation and RIA

The hypothalami, in acetic acid supplemented with a protease inhibitor, were heated at 95°C for 15 min, sonicated, and cell disruption was performed using a Dounce homogenizer. Samples were then centrifuged at 15000rpm at 4°C for 30 min. Finally, supernatants were collected and protein concentrations were determined by Bradford assay (Coomassie Protein Assay Reagent, Pierce. Rockford, IL, USA). Supernatants were then evaporated using a speed vacuum and reconstituted in 1 ml of 0.1% trifluoracetic acid (TFA) solution. 200 μg of total protein was injected into a Varian ProStar Gradient HPLC System equipped with a C18 reverse phase column (Microsorb MV 300-5; Varian Inc. Palo Alto, CA, USA) used to fractionate the tissue samples. For POMC-derivate peptide elution, a linear gradient was used from 20%–40% B in 20 min using the following mobile phases: (A) 0% acetonitrile/0.1% TFA and (B) 100% acetonitrile/0.1% TFA. The flow rate was 1.5 ml/min and there were equilibration times used on either side of the gradient. Fractions (0.75 ml) were collected over the entire 20 min gradient. These fractions were then evaporated using a speed vacuum and reconstituted in buffer used for RIA. Synthetic peptides were injected on the HPLC to determine retention times. Predicted retention times allowed for analysis of specific regions along the gradient for RIA analysis.

The assays used for α-MSH and ACTH-derived peptides were developed in our laboratory (E.N.) using commercially available peptides and primary antibodies. Each purified peptide was iodinated with ^{125}I using the Chloramine T oxidation-reduction method, purified by HPLC, and used as tracer. The α-MSH RIA was performed in 0.5 ml of phosphate buffer (pH 7.4)/500 mg/liter sodium azide/2.5 g/liter BSA, with primary anti-α-MSH antiserum (1:20,000), and 5000 cpm of ^{125}I des-αMSH tracer. The sensitivity of the assays was approximately 11.5 pg/tube, and the intra- and interassay variability were approximately 5%–7% and 10%–11%, respectively. The α-MSH assay used in this condition can detect both acetyl- and des-α-MSH forms. The ACTH RIA was also performed in 0.5 ml of the same RIA buffer by using the anti-ACTH antiserum (1:30,000) and 5000 cpm of ^{125}I-ACTH tracer. The sensitivity of the assays was approximately 10.0 pg/tube, and the intra- and interassay variability were approximately 5%–7% and 10%–11%, respectively.

Statistical Analysis

All values are expressed as mean ± SEM. Data were analyzed by two-way analysis of variance (ANOVA) for body weight change over time, calorie intake over time, i.p./i.c.v leptin effect on food intake, body weight, mRNA expression, IHC cell counts, and i.p./i.c.v. MTII effect on food intake. One-way ANOVA was used for final body weights, total calorie intake, feeding efficiency, blood leptin levels, and leptin sensitivity, followed by Bonferroni's Multiple Comparison Test. Body weight change correlation was analyzed using linear regression test. Secretion experiments were analyzed using Nonlinear Regression (sigmoidal dose-response best-fit curve). Data for the bimodal distribution was assessed by the D'Agostino & Pearson omnibus normality test. For glucose and insulin tolerance tests, areas under the curve (AUC) were calculated by trapezoid analysis and were compared by one-way ANOVA. Probability values < 0.05 were considered statistically significant. Analyses were performed with statistical software (GraphPad Prism 4.0, GraphPad Software, Inc., San Diego, CA).

Supplemental Data

Supplemental Data include three figures and can be found with this article online at http://www.cellmetabolism.org/cgi/content/full/5/3/181/DC1/.

ACKNOWLEDGMENTS

We wish to thank Drs. J.K. Elmquist, R.A. Batterham, J.A. Harrold, and G. Williams. Work supported by the following grants: P.J.E. (TW/HD-00668), E.A.N. (NIDDK/NIH R01 DK 58148, NINDS/NIH R01 NS 045231), K.L.G. (DK 60685 NIH RR 0163), and M.A.C. (NIH DK 62202, NIH RR 0163).

Received: October 4, 2006
Revised: February 1, 2007
Accepted: February 13, 2007
Published: March 6, 2007

REFERENCES

Balthasar, N., Coppari, R., McMinn, J., Liu, S.M., Lee, C.E., Tang, V., Kenny, C.D., McGovern, R.A., Chua, S.C., Jr., Elmquist, J.K., and Lowell, B.B. (2004). Leptin receptor signaling in POMC neurons is required for normal body weight homeostasis. Neuron *42*, 983–991.

Banks, W.A. (2003). Is obesity a disease of the blood-brain barrier? Physiological, pathological, and evolutionary considerations. Curr. Pharm. Des. *9*, 801–809.

Bates, S.H., Stearns, W.H., Dundon, T.A., Schubert, M., Tso, A.W., Wang, Y., Banks, A.S., Lavery, H.J., Haq, A.K., Maratos-Flier, E., et al. (2003). STAT3 signalling is required for leptin regulation of energy balance but not reproduction. Nature *421*, 856–859.

Bjorbaek, C., Elmquist, J.K., Frantz, J.D., Shoelson, S.E., and Flier, J.S. (1998). Identification of SOCS-3 as a potential mediator of central leptin resistance. Mol. Cell *1*, 619–625.

Breen, T.L., Conwell, I.M., and Wardlaw, S.L. (2005). Effects of fasting, leptin, and insulin on AGRP and POMC peptide release in the hypothalamus. Brain Res. *1032*, 141–148.

Burcelin, R., Crivelli, V., Dacosta, A., Roy-Tirelli, A., and Thorens, B. (2002). Heterogeneous metabolic adaptation of C57BL/6J mice to high-fat diet. Am. J. Physiol. Endocrinol. Metab. *282*, E834–E842.

Chen, H., Charlat, O., Tartaglia, L.A., Woolf, E.A., Weng, X., Ellis, S.J., Lakey, N.D., Culpepper, J., Moore, K.J., Breitbart, R.E., et al. (1996). Evidence that the diabetes gene encodes the leptin receptor: identification of a mutation in the leptin receptor gene in db/db mice. Cell *84*, 491–495.

Commins, S.P., Marsh, D.J., Thomas, S.A., Watson, P.M., Padgett, M.A., Palmiter, R., and Gettys, T.W. (1999). Norepinephrine is required for leptin effects on gene expression in brown and white adipose tissue. Endocrinology *140*, 4772–4778.

Cone, R.D. (2005). Anatomy and regulation of the central melanocortin system. Nat. Neurosci. *8*, 571–578.

Considine, R.V., Sinha, M.K., Heiman, M.L., Kriauciunas, A., Stephens, T.W., Nyce, M.R., Ohannesian, J.P., Marco, C.C., McKee, L.J., Bauer, T.L., et al. (1996). Serum immunoreactive-leptin concentrations in normal-weight and obese humans. N. Engl. J. Med. *334*, 292–295.

Coppari, R., Ichinose, M., Lee, C.E., Pullen, A.E., Kenny, C.D., McGovern, R.A., Tang, V., Liu, S.M., Ludwig, T., Chua, S.C., Jr., et al. (2005). The hypothalamic arcuate nucleus: a key site for mediating leptin's effects on glucose homeostasis and locomotor activity. Cell Metab. *1*, 63–72.

Cowley, M.A., Smart, J.L., Rubinstein, M., Cerdan, M.G., Diano, S., Horvath, T.L., Cone, R.D., and Low, M.J. (2001). Leptin activates anorexigenic POMC neurons through a neural network in the arcuate nucleus. Nature *411*, 480–484.

de Luca, C., Kowalski, T.J., Zhang, Y., Elmquist, J.K., Lee, C., Kilimann, M.W., Ludwig, T., Liu, S.M., and Chua, S.C. (2005). Complete rescue of obesity, diabetes, and infertility in db/db mice by neuron-specific LEPR-B transgenes. J. Clin. Invest. *115*, 3484–3493.

El-Haschimi, K., Pierroz, D.D., Hileman, S.M., Bjorbaek, C., and Flier, J.S. (2000). Two defects contribute to hypothalamic leptin resistance in mice with diet-induced obesity. J. Clin. Invest. *105*, 1827–1832.

Elias, C.F., Aschkenasi, C., Lee, C., Kelly, J., Ahima, R.S., Bjorbaek, C., Flier, J.S., Saper, C.B., and Elmquist, J.K. (1999). Leptin differentially regulates NPY and POMC neurons projecting to the lateral hypothalamic area. Neuron *23*, 775–786.

Elmquist, J.K., Bjorbaek, C., Ahima, R.S., Flier, J.S., and Saper, C.B. (1998). Distributions of leptin receptor mRNA isoforms in the rat brain. J. Comp. Neurol. *395*, 535–547.

Grove, K.L., Brogan, R.S., and Smith, M.S. (2001). Novel expression of neuropeptide Y (NPY) mRNA in hypothalamic regions during development: region-specific effects of maternal deprivation on NPY and Agouti-related protein mRNA. Endocrinology *142*, 4771–4776.

Halaas, J.L., Gajiwala, K.S., Maffei, M., Cohen, S.L., Chait, B.T., Rabinowitz, D., Lallone, R.L., Burley, S.K., and Friedman, J.M. (1995). Weight-reducing effects of the plasma protein encoded by the obese gene. Science *269*, 543–546.

Howard, J.K., Cave, B.J., Oksanen, L.J., Tzameli, I., Bjorbaek, C., and Flier, J.S. (2004). Enhanced leptin sensitivity and attenuation of diet-induced obesity in mice with haploinsufficiency of Socs3. Nat. Med. *10*, 734–738.

Huang, X.F., Han, M., South, T., and Storlien, L. (2003). Altered levels of POMC, AgRP and MC4-R mRNA expression in the hypothalamus and other parts of the limbic system of mice prone or resistant to chronic high-energy diet-induced obesity. Brain Res. *992*, 9–19.

Irani, B.G., Dunn-Meynell, A.A., and Levin, B.E. (2007). Altered hypothalamic leptin, insulin, and melanocortin binding associated with moderate-fat diet and predisposition to obesity. Endocrinology *148*, 310–316.

Kievit, P., Howard, J.K., Badman, M.K., Balthasar, N., Coppari, R., Mori, H., Lee, C.E., Elmquist, J.K., Yoshimura, A., and Flier, J.S. (2006). Enhanced leptin sensitivity and improved glucose homeostasis in mice lacking suppressor of cytokine signaling-3 in POMC-expressing cells. Cell Metab. *4*, 123–132.

King, P.J., Widdowson, P.S., Doods, H., and Williams, G. (2000). Regulation of neuropeptide Y release from hypothalamic slices by melanocortin-4 agonists and leptin. Peptides *21*, 45–48.

Koza, R.A., Nikonova, L., Hogan, J., Rim, J.S., Mendoza, T., Faulk, C., Skaf, J., and Kozak, L.P. (2006). Changes in gene expression foreshadow diet-induced obesity in genetically identical mice. PLoS Genet *2*, e81. 10.1371/journal.pgen.0020081.

Levin, B.E., Dunn-Meynell, A.A., Balkan, B., and Keesey, R.E. (1997). Selective breeding for diet-induced obesity and resistance in Sprague-Dawley rats. Am. J. Physiol. *273*, R725–R730.

Li, G., Zhang, Y., Wilsey, J.T., and Scarpace, P.J. (2004). Unabated anorexic and enhanced thermogenic responses to melanotan II in diet-induced obese rats despite reduced melanocortin 3 and 4 receptor expression. J. Endocrinol. *182*, 123–132.

Li, J.Y., Finniss, S., Yang, Y.K., Zeng, Q., Qu, S.Y., Barsh, G., Dickinson, C., and Gantz, I. (2000). Agouti-related protein-like immunoreactivity: characterization of release from hypothalamic tissue and presence in serum. Endocrinology *141*, 1942–1950.

Lin, S., Storlien, L.H., and Huang, X.F. (2000a). Leptin receptor, NPY, POMC mRNA expression in the diet-induced obese mouse brain. Brain Res. *875*, 89–95.

Lin, S., Thomas, T.C., Storlien, L.H., and Huang, X.F. (2000b). Development of high fat diet-induced obesity and leptin resistance in C57Bl/6J mice. Int. J. Obes. Relat. Metab. Disord. *24*, 639–646.

Liu, H., Kishi, T., Roseberry, A.G., Cai, X., Lee, C.E., Montez, J.M., Friedman, J.M., and Elmquist, J.K. (2003). Transgenic mice expressing green fluorescent protein under the control of the melanocortin-4 receptor promoter. J. Neurosci. *23*, 7143–7154.

Mori, H., Hanada, R., Hanada, T., Aki, D., Mashima, R., Nishinakamura, H., Torisu, T., Chien, K.R., Yasukawa, H., and Yoshimura, A. (2004). Socs3 deficiency in the brain elevates leptin sensitivity and confers resistance to diet-induced obesity. Nat. Med. *10*, 739–743.

Munzberg, H., Flier, J.S., and Bjorbaek, C. (2004). Region-specific leptin resistance within the hypothalamus of diet-induced obese mice. Endocrinology *145*, 4880–4889.

Munzberg, H., and Myers, M.G., Jr. (2005). Molecular and anatomical determinants of central leptin resistance. Nat. Neurosci. *8*, 566–570.

Nillni, E.A., Vaslet, C., Harris, M., Hollenberg, A., Bjorbak, C., and Flier, J.S. (2000). Leptin regulates prothyrotropin-releasing hormone biosynthesis. Evidence for direct and indirect pathways. J. Biol. Chem. *275*, 36124–36133.

Parekh, P.I., Petro, A.E., Tiller, J.M., Feinglos, M.N., and Surwit, R.S. (1998). Reversal of diet-induced obesity and diabetes in C57BL/6J mice. Metabolism *47*, 1089–1096.

Paxinos, G., and Franklin, K.B.J. (2001). The Mouse Brain in Stereotaxic Coordinates (San Diego: Academic Press).

Pierroz, D.D., Ziotopoulou, M., Ungsunan, L., Moschos, S., Flier, J.S., and Mantzoros, C.S. (2002). Effects of acute and chronic administration of the melanocortin agonist MTII in mice with diet-induced obesity. Diabetes *51*, 1337–1345.

Pritchard, L.E., Oliver, R.L., McLoughlin, J.D., Birtles, S., Lawrence, C.B., Turnbull, A.V., and White, A. (2003). Proopiomelanocortin-derived peptides in rat cerebrospinal fluid and hypothalamic extracts: evidence that secretion is regulated with respect to energy balance. Endocrinology *144*, 760–766.

Rosenbaum, M., Goldsmith, R., Bloomfield, D., Magnano, A., Weimer, L., Heymsfield, S., Gallagher, D., Mayer, L., Murphy, E., and Leibel, R.L. (2005). Low-dose leptin reverses skeletal muscle, autonomic, and neuroendocrine adaptations to maintenance of reduced weight. J. Clin. Invest. *115*, 3579–3586.

Sahu, A., Nguyen, L., and O'Doherty, R.M. (2002). Nutritional regulation of hypothalamic leptin receptor gene expression is defective in diet-induced obesity. J. Neuroendocrinol. *14*, 887–893.

Schmidt, I., Schoelch, C., Ziska, T., Schneider, D., Simon, E., and Plagemann, A. (2000). Interaction of genetic and environmental programming of the leptin system and of obesity disposition. Physiol. Genomics *3*, 113–120.

Schwartz, M.W., Seeley, R.J., Campfield, L.A., Burn, P., and Baskin, D.G. (1996). Identification of targets of leptin action in rat hypothalamus. J. Clin. Invest. *98*, 1101–1106.

Schwartz, M.W., Seeley, R.J., Woods, S.C., Weigle, D.S., Campfield, L.A., Burn, P., and Baskin, D.G. (1997). Leptin increases hypothalamic pro-opiomelanocortin mRNA expression in the rostral arcuate nucleus. Diabetes *46*, 2119–2123.

Seeley, R.J., and Woods, S.C. (2003). Monitoring of stored and available fuel by the CNS: implications for obesity. Nat. Rev. Neurosci. *4*, 901–909.

Spiegelman, B.M., and Flier, J.S. (2001). Obesity and the regulation of energy balance. Cell *104*, 531–543.

Takahashi, N., Patel, H.R., Qi, Y., Dushay, J., and Ahima, R.S. (2002). Divergent effects of leptin in mice susceptible or resistant to obesity. Horm. Metab. Res. *34*, 691–697.

Tschop, M., and Heiman, M.L. (2001). Rodent obesity models: an overview. Exp. Clin. Endocrinol. Diabetes *109*, 307–319.

van den Top, M., Lee, K., Whyment, A.D., Blanks, A.M., and Spanswick, D. (2004). Orexigen-sensitive NPY/AgRP pacemaker neurons in the hypothalamic arcuate nucleus. Nat. Neurosci. *7*, 493–494.

Wang, H., Storlien, L.H., and Huang, X.F. (2002). Effects of dietary fat types on body fatness, leptin, and ARC leptin receptor, NPY, and AgRP mRNA expression. Am. J. Physiol. Endocrinol. Metab. *282*, E1352–E1359.

Wilson, B.D., Bagnol, D., Kaelin, C.B., Ollmann, M.M., Gantz, I., Watson, S.J., and Barsh, G.S. (1999). Physiological and anatomical circuitry between Agouti-related protein and leptin signaling. Endocrinology *140*, 2387–2397.

Zamboni, M., Mazzali, G., Zoico, E., Harris, T.B., Meigs, J.B., Di Francesco, V., Fantin, F., Bissoli, L., and Bosello, O. (2005). Health consequences of obesity in the elderly: a review of four unresolved questions. Int. J. Obes. (Lond.) *29*, 1011–1029.

Zhang, Y., and Scarpace, P.J. (2006). The role of leptin in leptin resistance and obesity. Physiol. Behav. *88*, 249–256.